摘要

粒線體在細胞的存活與死亡上扮演著重要的角色。粒線體擁有的遺傳物質，能夠轉譯出粒線體呼吸鏈所需要的次單元體。粒線體的遺傳物質(mtDNA)的突變和大部份的神經性、肌肉性疾病相關。肌陣攣癲癇是一種母系遺傳的粒線體疾病。而導致這種疾病發生的主要原因是在 mtDNA 上第 A8344G 的位置上產生點突變所造成的，而嚴重影響粒線體的蛋白質合成，並且進一步的損害粒線體電子傳遞鏈的組裝以及呼吸鏈的活性。在我們先前的實驗結果中發現熱休克蛋白 27 的表現量，不論是在 MERRF 病人的淋巴母細胞中或是帶有 mtDNA A8344G 點突變的融合細胞株當中都有顯著下降的情形。而在帶有突變 mtDNA 的融合細胞株中，大量表現熱休克蛋白 27 能夠有效的減少 staurosporine 所活化的 caspase 3，而顯示了熱休克蛋白 27 在帶有 mtDNA A8344G 點突變的融合細胞中具有保護的作用。目前的結果中，磷酸化的熱休克蛋白 27 於突變的融合細胞中顯著的下降。然而磷酸化的熱休克蛋白 27 在正常情況下表現量雖然較低，但在受到壓力的處理時，磷酸化以及去磷酸化的表現和野生型融合細胞，顯示激酶和去磷酸酶的活性表現皆正常。接著我們進一步的檢視磷酸化熱休克蛋白 27 於疾病的細胞模型中的保護功能。利用 3 個 Serine 磷酸化

位點同時突變成 Asparagine 的熱休克蛋白 27 來模擬持續磷酸化表現的熱休克蛋白 27，透過短暫性轉染後，發現模擬磷酸化表現的熱休克蛋白 27 對於 staurosporine 所引發的細胞凋亡較不敏感。細胞在受到熱休克處理之後，磷酸化熱休克蛋白 27 會迅速的進入細胞核中，再給予不同長度的恢復時間後，控制組的磷酸化熱休克蛋白 27 會較快速地由細胞核回到細胞質中表現，但在突變的細胞中則否。並且，這個磷酸化熱休克蛋白 27 易位現象和細胞存活度是有相關性的。目前，我們的結果說明了在 MERRF 疾病的細胞模型當中，磷酸化的熱休克蛋白 27 在各種不同的壓力處理下都提供了保護的功能。因此，我們相信在醫療策略上若是能夠提高磷酸化熱休克蛋白 27 的表現也許能夠提供疾病另一種具有潛力的治療方式。

Abstract

Mitochondria play an important role in the life and death of cells. They have their own DNAs which encode subunits of mitochondrial electron transport chain complexes. Mitochondrial DNA mutations are associated with a large number of neurological and muscular diseases. Myoclonus Epilepsy with Ragged Red Fibers (MERRF) is a maternal inheritance mitochondrial disease. The most common mutation in MERRF disease, A8344G, is associated with severe defects in mitochondrial protein synthesis, which impairs electron transport chain assembly and respiratory chain activity. We have previously shown that a decreased level of heat shock protein 27 (HSP27) in lymphoblastoid cells derived from a MERRF patient and in cybrids harboring MERRF A8344G mutation. Over-expressed wild type HSP27 in mutated cybrids resulted in a significant decrease of activated caspase 3 under staurosporine (STS) treatment, suggesting a protective function of HSP27 in cells harboring MERRF mutation. In the present study, we reported a dramatic decreased level of phospho-HSP27 in the mutant cybrids. Even though the steady-state level of p-HSP27 was reduced in mutant cybrids, normal

phosphorylation and dephosphorylation responses were observed upon stresses, indicating normal kinase and phosphatase activities. We next examined the protective function of p-HSP27 in the disease cellular model. To explore the roles that p-HSP27 may play, transfection experiments with HSP27 mutants, in which three specific serine residues were substituted with alanines or aspartic acids, showed that the phosphomimicking-HSP27 desensitized mutant cybrids to apoptotic stress induced by STS. After heat shock stress, p-HSP27 entered the nucleus immediately after heat shock. With prolonged recovery intervals after heat shock, p-HSP27 returned to the cytoplasm in normal cybrids but not in mutant cybrids and this translocation is correlated to cell viability, as evidenced by the increased apoptotic cells after p-HSP27 returning to the cytoplasm. In summary, our results demonstrate that p-HSP27 provides significant protective functions when cells are under different stresses in the MERRF disease cellular model. Therapeutic strategies against anomalous HSP27 phosphorylation might be a potential treatment for the disease.

Introduction

Mitochondria are important intracellular organelles in eukaryotic cells, harboring their own genetic materials called mitochondrial DNA (mtDNA). The main role of mitochondria is to synthesize ATP, which provides the universal energy source for cells. Because of different cell types, the numbers of mitochondria differ from hundreds to thousands per cell. Various mtDNA mutations lead to mitochondrial dysfunctions and cause human neuromuscular diseases. However, the defective mitochondrial function is represented only when a threshold of mtDNA mutation rate in the cells is reached (Hammans et al., 1993; Chinnery et al., 1997; Rossignol et al., 2003). mtDNA encodes 13 polypeptides which are the subunits of respiration complexes. However, most of the proteins assembled into functional complexes are encoded by nuclear DNA (nDNA). Therefore, the nDNA mutation may also affect the normal functions of mitochondria. Mitochondrial diseases are classified as different syndromes, according to the clinical symptoms. Myoclonus Epilepsy associated with Ragged-Red Fibers disease (MERRF), chronic progressive external ophthalmoplegia syndrome (CPEO) and

mitochondrial encephalomyopathy, lactic acidosis and strokelike episodes (MELAS) are commonly caused by pointed mutations or large- scale deletions of mtDNA (Schon et al., 1997).

Myoclonus Epilepsy associated with Ragged-Red Fibers disease (MERRF)

MERRF syndrome caused by mtDNA mutations is a maternal inheritance encephalomyopathy. The pathogenesis of MERRF is due to point mutations in *mt-tRNA*^{Lys} gene at A8344G, T8356C or G8363A. These mutations lead to translational dysfunction and finally affect mitochondrial activity (Antonicka et al., 1999). The most common mutation site is an A to G transition at nucleotide 8344 (A8344G) in the *tRNA*^{Lys}. In the mutated cells, both the oxygen consumption of electron transport chain (ETC) and the respiratory chain activity are decreased (Yoneda et al., 1994). The nt 8344 mutation has been associated with severe defects in protein synthesis, which leads to a general decrease in respiration rate and oxygen consumption in cells and tissue mitochondria (Arpa et al., 1997; James et al., 1996; Larsson et al., 1992; Yoneda et al., 1994). Previous studies have reported that the activity of cytochrome *c*

oxidase (cox) in MERRF patient's fibroblasts with 89% mutant mtDNA was decreased to 20% of the control level, the amount of ATP synthesis was decreased to 50 % and the mitochondrial membrane potential retained only 20 % compared with the control cells (Boulet et al., 1992). In addition, it is known that the large amount of reactive oxygen species (ROS) is detected in mutant cells which lead to an increased oxidative stress. (Boulet et al., 1992; Larsson et al., 1992; Wei et al., 1996; Antonicka et al., 1999)

When cells are under stress conditions, including heat, oxidative stress, ischemia or bacterial endotoxins, rapid production of the important protein family called heat shock protein (HSPs) is well documented (Arya et al., 2007; Concannon et al., 2003). HSPs are a group of stress responsible proteins in cells (Welch, 1993). Stress stimulated *HSP* gene activation is mediated by the interaction of heat shock element (HSE) and heat shock factor (HSF) (Pirkkala et al., 2001; Morano and Thiele, 1999). The heat shock protein family members are divided into two subgroups: the high molecular weight heat shock proteins and the small heat shock proteins. All the HSPs are known to function as molecular chaperones

that help other proteins to adopt a functional conformation. The high molecular weight heat shock proteins, such as HSP110, HSP90, HSP70 are ATP-dependent and the small heat shock proteins, such as HSP32, HSP27, αB-crystallin are ATP-independent (Jakob et al., 1993; Ghosh et al., 2011). The ATP-independent chaperone proteins prevent the mis-folded proteins from aggregation and maintain their solubility until other ATP-dependent chaperones to help them re-fold back to the correct conformation (Ehrnsperger et al., 1997; MacRae, 2000).

HSP27 is a member of sHSP family which share sequence homologies and biochemical properties such as phosphorylation and oligomerization (Arrigo et al., 1994). It is known that HSP27 functions as a molecular chaperone and also a negative regulator of apoptosis. When cells are under stresses, HSP27 performs its chaperone ability to preserve the solubility of the denatured proteins or the mis-folded proteins by integration with them directly (Concannon et al., 2003). Moreover, HSP27 protects against apoptotic cell death triggered by stimuli including hyperthermia, oxidative, Fas ligand, straurosporine, and cytotoxic drugs (Arya et al., 2007; Concannon et al., 2003). Apoptotic cell death can be

mediated by two major pathways, either involving the mitochondria (intrinsic) or the Fas protein (extrinsic). In the intrinsic apoptotic pathway, HSP27 blocks the activation of apoptosis initiating factors (AIFs) through inhibiting Bax activation or directly interacts with cytochrome *C* to inhibit the caspase cascade and down regulates the apoptosis activation (Garrido et al., 1999; Bruey et al., 2000; Pandey et al., 2000). In the extrinsic apoptotic pathway, HSP27 interacts with DAXX to reduce cell death upon apoptosis stresses (Charette et al., 2000). There are three main domains in the structure of HSP27, which are WDPF domain, α-crystallin domain and flexible domain. The WDPF domain is used for small aggregate formation, the α-crystallin domain is for large polymer formation and the flexible domain helps retain its solubility. There are many pieces of evidence that phosphorylation or changes in the supermolecular organization modulate the activity of HSP27 (Kosten and Moens, 2009). The phosphorylatable serine residues appear to be the key elements affecting HSP27 structural organization and the interaction with other cytoskeletal elements (Hickey et al., 1986; Loktionova and Kabakov, 2001).

HSP27 contains three major phosphorylation sites, including Ser-15,

Ser-78 and Ser-82 respectively. It is known that HSP27 are phosphorylated by MAPKAP kinase 2/3 and dephosphorylated by Protein phosphatase 2 (PP2A) which is ubiquitously expressed is a serine/threonine phosphatase (Cairns et al., 1994; Berrou and Bryckaert, 2009). HSP27 formed large polymers but phosphorylated HSP27 (p-HSP27) showed a tendency to form dimers or tetramers (Kosten and Moens, 2009). It has been demonstrated that such a rapid induction of p-HSP27 stabilizes the cytoskeleton through binding to the F-actin when cells are under oxidative stress (Tak et al., 2007). In addition, the transient up-regulation of p-HSP27 not only enhances the thermoresistance but also provides a protective function under oxidative stress (Geum et al., 2002; Storz and Stoker, 2003). A recent study showed that p-HSP27, through stabilizing the serine/threonine-specific protein kinase (Akt or PKB), up-regulates the phosphorylated p21 to increase the cell viability in the normal growth condition. On the other hand, under UV irradiation, p-HSP27 interacts with p53, facilitates its degradation and finally inhibits cell apoptosis (Kanagasabai et al., 2010). Moreover, it has been suggested that the translocation of p-HSP27 from the cytoplasm to the nucleus may function to protect nuclear DNA breakdown (Geum et al., 2002). Other

studies also indicated that p-HSP27 inhibited translation through binding eukaryotic translation initiation factor 4 gamma (eIF4G) (Cuesta et al., 2000). Moreover, it was demonstrated that p-HSP27 enters the nucleus and blocks the MAPK/ERK kinase (MEK)/ extracellular-signal-regulated kinases (ERK) pathway, which results in the down-regulation of cyclin D1 and cell cycle arrest under tumor necrosis factors α (TNFα) treatment (Matsushima et al., 2008). Our previous results have demonstrated that the protein expression levels of HSP27 and p-HSP27 were markedly decreased in cells harboring MERRF A8344G mutation (Chen et al., 2011). In the present study, we further examined whether the over-expressed HSP27 in MERRF cybrids offers a protective function on cell viability under stress conditions. In addition, the roles of p-HSP27 may play in the disease cellular model were also investigated.

Material and method

Cell culture

MERRF cybrids were kindly provided by Dr. Wei YH at Yung-Ming University. C5 cybrids harbor almost 100 % A8344G mutation mtDNA. D5-1 cybrids contain almost 100 % wild type mtDNA. These two cybrids are with the same genetic background. C5-C5 and C6 are the wild type HSP27 expression stable cell lines with C5 background (Chen et al., 2011). Cells were sub-cultured in 25T flask and passaged 2 to 3 times per week. Cells were maintained in Dulbecco's modified eagle's medium (DMEM) containing pyruvate and uridine (Dulbecco's modified eagle's medium: 1 % non-essential amino acid, 1 % penicillin-streptomycin, 1 % L-glutamine、10 % fetal bovine serum, 100 ug/ml pyruvate and 50 ug/ml uridine, represent as P+U+ DMEM) at 37°C in an atmosphere of 5% CO_2 and 95 % air. For the following experiment, cells were seeded in DMEM without pyruvate and uridine (represent as P-U- DMEM) for 48hr before further treatment.

Heat-shock treatment

Cybrid cells were seeded at 3 x 10^5 cells in 3 cm tissue culture dishes and incubated for 48 h in P-U- DMEM at 37°C, 5% CO_2 incubator; heat shocked by incubating in a water bath for 30 min at 43℃; and allowed to recover for 0, 10, 20, 30 and 60 min at 37℃. For the maximum production of p-HSP27, cells were heat shocked at 43℃ for 30 min and recovered for 1, 3, 5, 7 and 9 hr before assaying the cellular distribution of p-HSP27 and cell viability.

STS treatment

To induce cells to undergo apoptosis, we seeded cells at 3 x 10^5 cells in 3 cm tissue culture plates and incubated for 48 h in P-U- DMEM at 37°C, 5% CO_2 incubator to obtain monolayer cultures. After cybrid cells were treated with 300 nM STS for 3 h, cells on coverslips were fixed with 4% paraformaldehyde and mounted in phosphate buffered saline with 0.1 % Tween 20 (PBST) with propidium iodide (PI) (20 μg/ml) to allow visualization of the nuclear morphology.

Oxidative stress

Cells were seeded at 3 x 10^5 cells in 3 cm tissue culture plates and incubated for 48 h in P-U- DMEM at 37°C, 5% CO_2 incubator to obtain monolayer cultures. After cybrid cells were treated with 90 μ M H_2O_2 for 60 min, cells on coverslips were fixed with 4% paraformaldehyde and mounted in phosphate buffered saline with 0.1 %, Tween 20 (PBST) with propidium iodide (PI) (20 μg/ml) and rabbit-anti-pHSP27 (1:200) allow visualization the cellular distributation.

Cell lysates for SDS-PAGE

Cells were washed three times with phosphate buffered saline (PBS, pH 7.2), resuspended in 500 μl of lysis buffer (5% glycerol, 1X PBS, 0.5 % triton X-100, 1X protease inhibitor, 1 mM sodium EDTA, 1 mM sodium EGTA, 1 mM dithiothreitol), for phosphorylated proteins the 1 mM PMSF, 1 mM Na_3VO_4, 1μg/ml Aprotintin and 2μg/ml Leupeptin added additionally then incubated on ice for 15 min. After scratching the resultant cell lysate was centrifuged at 13200 rpm for 15 min at 4℃. Supernatant was collected, and Bio-Rad protein assay reagent was used to determine the protein concentrations.

DNA fragmentation assay

Cells were seeded at 3 x 10^5 cells in 3 cm tissue culture plates and incubated for 48 h in P-U- DMEM at 37°C, 5% CO_2 incubator to obtain monolayer cultures. After cybrid cells were treated with 90 μ M H_2O_2 for 60 min, cells were harvested and centrifuged at 4000rpm for 10min.

The cells were pelleted and resuspended in 100 µL of the lysis buffer (1% NP-40, 20 mM EDTA, 50 mM Tris-HCl, pH 7.5). After incubation at 4°C for 20 s, cells were centrifuged at 900g for 5 min at 4°C. The supernatant was added with RNase A (final concentration of 5 µg/µL) and SDS (final concentration of 1%), and the mixture was incubated for 2 h at 56°C. Proteinase K was added to the supernatant (final concentration of 2.5 µg/µL) and incubated for 4 h at 37°C. After adding 2.5 volumes of ethanol and 1/10 volume of 3 M sodium acetate, the solution was stored at –20°C for more than 8 h to precipitate DNA. DNA was collected by centrifugation at 9,000g for 30 min at 4°C, and washed by 70% cool ethanol and air-dried. The DNA pellet then was dissolved in distilled H2O and subjected to electrophoresis on a 2% agarose gel.

Western blotting

In brief, cell lysates containing 30 μg of protein were loaded onto 10 or 12% sodium dodecyl sulfate (SDS)-polyacrylamide gels. Resolved proteins were electrophoretically transferred onto 0.2 μm PVDF membranes. After blocking the membrane with 5% nonfat milk in TTBS buffer for 1 h at room temperature (or 5% BSA for phosphorylated protein), the antibody-binding reactions were performed in the same buffer supplemented with 5% nonfat milk (or 5% BSA for phosphorylated protein) at 4℃ overnight or at room temperature for 1 h in order for secondary antibodies to couple to horseradish peroxides (HRP)-conjugated anti-goat IgG. Prestained high molecular weight markers were included in this study. Signals were visualized with the enhanced chemiluminescence. Protein bands were quantitated by densitometry, and protein loading was normalized with β-actin or α-tubulin. For quantitation of proteins levels, the amount of protein loaded on the gel was optimized, and multiple exposures were performed to ensure that the signals were within the linear response range.

Transient transfection

Transient-transfection was performed in exponentially growing cells that were plated one day before transfection in 3 cm dishes (5×10^5cells/well). 1μg of plasmid DNA (pcDNA3-HA-HSP27-S3A, pcDNA3-HA-HSP27-S3D, pcDNA3.1- HSP27 -myc-His, pcDNA3.1 -myc-His were transfected according to experiment needed) with 5 μl of Lipofectamine and 8 μl of Plus reagent (Invitrogen-Life Technologies) which were preincubated for 30 minutes and then added to the cells. After 4 hours, the Optimum DNA mixture was replaced with complete growth medium, and 24 hours later cells were harvested after experiment treatment.

Immuno-fluorescence staining

Cybrid cells were seeded on the cover slides at 3×10^5 cells/well in 3 cm tissue culture dishes and incubated for 48 h in P-U- DMEM at 37°C, 5% CO_2 incubator. Then cells were washed three times with 1X PBS, and fixed with 4 % paraformaldehyde / 1x PBS (PH = 7.2) for 30 minutes in room temperature. After washing with PBST (0.2% Triton X- 100 in 1X PBS), cells were blocked with 10 % fetal bovine serum and incubated

with primary antibodies for 16 hr to 18 hr at 4°C. Following incubation, cells were washed three times with 1X PBST and then incubated with the corresponding secondary antibodies for 2 h at room temperature. Coverslides were washed three times, incubated with propidium iodide (PI) for 10 min, washed three times, and mounted by glycerol.

The images were captured by Olympus laser-scanning confocal microscope. 1° Ab final concentration (containing RNAseA 20μg/ml): mouse-anti-cMyc (1: 200), goat-anti- HSP27 (1:200), rabbit-anti-pHSP27 (1:200), mouse-anti-HA (1:200). 2° Ab final concentration: Donkey-anti-mouse-FITC (1:200), Goat-anti-rabbit-dylight 649 (1:200).

JC-1 staining

Cybrid cells were seeded on the cover slides at 3 x 10^5 cells/well in 3 cm tissue culture dishes and incubated for 48 h in P-U- DMEM at 37°C, 5% CO_2 incubator.

Then cells were washed three times with 1X PBS, stained with 1 μ g/ml JC-1 in P-U- DMEM at 37°C, 5% CO_2 incubator for 10 min. After staining, cells were mounted by glycerol and observed by Olympus

laser-scanning confocal microscope. JC-1 was excited with the 488 nm argon laser, and JC-1 green and orange flrgon laser, were recorded on 530 nm band pass filter and 575 nm band pass filter channels. All figures were taken by Olympus laser-scanning confocal microscope. The fluorescence intensity was measured by LSM510. The red/green fluorescence ratio indicated the mitochondrial membrane potential.

Statistical analysis

All bands in figures were quantified by laser densitometry and values are expressed as a mean ± standard error of the mean (SEM). Comparison between experimental groups was made using Student's *t* test. Values were considered significantly different if $p<0.05$.

3. Results

3.1. Dramatically decreased p- HSP27 expression in the presence of mutant MERRF

We have previously shown that the expression level of HSP27 in C5 (mutant) cybrids was decreased to about 40% of the wild type level (Appendix Fig. 1). Because HSP27 is also a phosphorylated protein which plays important roles in cell protection and viability, we then examined the level of p-HSP27 under the normal growth condition. It was noted that p-HSP27 in the mutant cells showed a more drastic decrease, with only 20% of that of the control cells (Appendix Fig. 1A and 1B). To understand whether the differential expression of p-HSP27 affects its cellular localization, we next examined the distribution of p-HSP27 under normal growth condition. As shown in Appendix Fig. 2, the cellular localization of HSP27 and p-HSP27 are evenly distributed in the cytoplasm under normal growth condition.

3.2. Low content of p-HSP27 in the mutant MERRF cybrids is not due to low content of ATP

Because there is a significant decrease of ATP synthesis in MERRF cells, we wonder whether the low ATP production leads to a general effect of decreased protein phosphorylation. To check the putative correlation of the p-HSP27 level and ATP content, Chronic Progressive External Ophthalmoplegia (CPEO) cybrids, which contained about 80% of 4977-bp deletion mtDNA (Liu et al., 2004), were used for comparison. It was shown previously that mitochondrial respiratory function in the 4977-bp deletion cybrids was decrease to 46% of that of the control (Liu et al., 2009). Western blotting showed an increased p-HSP27 in mutant CPEO cells compared to the normal control, suggesting that the lack of ATP production in mutant cells is not responsible for the decreased level of p-HSP27. Meanwhile, it is noted that the phosphorylated-ERK is not down-regulated in MERRF cybrids compared to the normal control cells (Appendix Fig. 3.). Taken together, these results suggest that the reduced levels of p-HSP27 are not due to the low content of ATP in cells harboring MERRF mutation.

3.3 The decreased p-HSP27 may not be due to defective kinase activity

To gain a more comprehensive understanding of the regulation of p-HSP27, we further examined whether the dramatic decreased p-HSP27 in C5 cybrids was due to the defective kinase activity. To estimate the kinase activity in cybrids, transient transfection was performed by using pcDNA3.1-HSP27-myc-his which carries C-terminal myc-his tagged HSP27. After transiently transfected into C5 and D5-1 cybrids, the protein levels of exo- pHSP27 and exo-HSP27 were detected by Western blot analysis. The ratio of exo-pHSP27 /exo-HSP27 was taken as an indication of the kinase activity under steady-state condition. Our results reveal no significant difference in the ratios of the exo-pHSP27 /exo-HSP27 between D5-1 and C5 cybrids (Fig. 1), indicating that the decreased p-HSP27 in mutant C5 was not due to the defective protein kinase activity.

3.4 The decreased p-HSP27 does not affect the normal stress response

It is known that the expression level of p-HSP27 increased under stress conditions (Gusev et al., 2002). To understand whether the decreased p-HSP27 in C5 cybrids affects stress response, protease inhibitor MG132 and heat shock treatments were performed accordingly. As shown in appendix Fig. 4, after MG132 treatment for 15 min, a strong increase of p-HSP27 was detected, indicating an immediate pharmacological response. However, the level of p-HSP27 decreased with prolonged incubation and increased again after 2 hr treatment in both D5-1 and C5 cybrids (Appendix Fig. 4), which is consistent with the accumulation of HSP70. Responses from HSP70 were detected for comparison because the degradation of HSP70 is blocked by proteasome inhibitor MG132 (Chen et al., 2011). The similar patterns of induced phosphorylated upon MG132 treatment and returned to basal level after 1 hour, indicating normal functions of kinase and phosphatase to regulate the phosphorylation status of HSP27. In addition, we further examined the response of p-HSP27 in both D5 and C5 cybrids under heat shock treatment. As expected, a significant increased p-HSP27 was observed at

a treatment for 60 min in both D5-1 and C5 cybrids (Fig. 2). Taken together, these results indicate that the decreased p-HSP27 did not affect the stress response.

3.5 Over-expression of HSP27 desensitizes mutant cybrids to apoptotic stress

It was previously shown that the cybrids harboring mutated mtDNA were more susceptible to apoptosis upon UV or STS treatment (Liu et al., 2004; Wu et al., 2010). Since mtDNA A8344G point mutation may exert pro-apoptotic effects through a down-regulation of HSP27, we further investigated whether over-expression of HSP27 desensitizes mutant MERRF cybrids to apoptotic stress. Mammalian expression plasmid pcDNA3.1-HSP27-myc-his was constructed previously (Chang et al., 2009) and stably transfected into C5 cybrids. Two stable lines, C5-C5 and C6, were obtained after G418 selection and the exogenous expression of wild-type HSP27 was confirmed by Western blot analysis (Fig. 3). We next analyzed the effects of over-expressed HSP27 in the presence of A8344G mutation. D5-1 and C5 cybrids, as well as C5-C5 and C6, were

treated with 300 nM STS for 3 hr and assayed for activated caspase 3 by Western blot analysis. As shown in Fig. 4, we observed a significant decrease of activated caspase-3 in C5-C5 and C6 compared with mutant C5 harboring no exogenous HSP27. Our results demonstrate that exogenous expression of wild type HSP27 desensitizes mutant cybrids to STS-induced apoptosis.

3.6 The over-expressed HSP27 does not rescue the decreased mitochondrial membrane potential in cybrids harboring A8344G mutation

Because an 80 % decrease of mitochondrial membrane potential was observed in patient fibroblast cells harboring 89 % A8344G mtDNA point mutation (Antonicka et al., 1999), we further used the HSP27 over-expression clone, C6, to assess whether the over-expressed HSP27 rescues the mitochondrial membrane potential in the mutant cybrids. Mitochondrial membrane potential was monitored by JC-1 dye. JC-1 has been widely used to analyze mitochondrial membrane potential because it is a lipophilic cationic fluorescence dye and shows two distinct

sub-populations with different mitochondrial membrane potential, red with high mitochondrial membrane potential and green with low mitochondrial membrane potential. After JC-1 staining, the ratio of red/green fluorescent intensity was taken as an indicator of the mitochondrial membrane potential. The D5-1 cybrids showed a significant higher mitochondrial membrane potential than that of C5 cybrids. However, the mitochondrial membrane potential was not significantly increased in the HSP27 over-expressed clone, C6, compared to C5 mutants (Fig. 5). Our results indicate that the over-expressed HSP27 in C6 cells does not rescue the decreased mitochondrial membrane potential in C5 mutant cells harboring A8344G mtDNA point mutation.

3.7 The phosphomimicking-HSP27 shows the ability to desensitize mutant cybrids to STS treatment

Human HSP27 is known to be phosphorylated at three serine residues (ser15, ser75 and ser82) (Gusev et al., 2002). In order to understand whether the phosphorylation of HSP27 plays important roles on cell

protection and viability in cells harboring A8344G point mutation, mammalian expression plasmids pcDNA3-HA-HSP27-S3A, with all three serine residues changed to alanine, and pcDNA3-HA-HSP27-S3D, with all three serine residues changed to aspartic acid, were constructed for comparison (Chen, unpublished data). The HSP27-S3A represents the non- phosphorylatable HSP27 and the HSP27-S3A is the phosphomimicking HSP27. We then examined the exogenous expression of the mutant forms of HSP27 by Western blot analysis. As shown in Fig. 6, the expression of HSP27-S3A and HSP27-S3D was confirmed. Next, we performed cell viability assay for assessment the protective function of the point mutated HSP27 in C5 cybrids harboring A8344G point mutation under apoptotic stress. Cells were transient transfected with plasmid HSP27-S3A, HSP27-S3D, HSP27-myc-his and LacZ control, followed by treated with 300nM STS for 3 hr. As shown in Fig. 7, wild-type HSP27-myc-his transfected cells showed a decreased cell death compared with that of the LacZ control. Interestingly, the S3D-HSP27 transfected cells showed a significant decrease of cell death under STS treatment when compared to that the S3A-HSP27 transfected cells. Our results demonstrate that the phosphomimicking-HSP27 showed the

ability to desensitize mutant cells to STS-induced apoptotic stress.

To further investigate the protective function of phosphomimicking-HSP27, another point mutated mitochondrial disease, MELAS was taken for comparison. At first, we examined the protein expression level of HSP27 and p-HSP27. As shown in Appendix Fig. 6, Both p-HSP27 and HSP27 showed a significant decrease in Lu04 (mutant) cybrids. Furthermore, after treatment with 100nM STS for 6hr the activated caspase 3 was increased in Lu04 which coincidence to the C5 cybrids (Fig.8). We further repeated the transient transfection with plasmid HSP27-S3A, HSP27-S3D, HSP27-myc-his and LacZ control, followed by treated with 100nM STS for 6 hr. As shown in Fig. 9, wild-type HSP27-myc-his transfected cells showed a decreased cell death compared with that of the LacZ control. The same result was observed, the S3D-HSP27 transfected cells showed a significant decrease of cell death under STS treatment when compared to that the S3A-HSP27 transfected cells. These results demonstrate that the phosphomimicking-HSP27 showed the ability to desensitize mutant cells to STS-induced apoptotic stress in both cells harboring MELAS and

MERRF mutation.

3.8 The translocation of p-HSP27 correlates with cell viability after heat shock stress

Our previous data have shown that the HSP27 and p-HSP27 were distributed in the cytoplasm evenly in both D5-1 and C5 cybrids (Appendix Fig. 2). It was reported previously that the HSP25, the mouse ortholog of human HSP27, was phosphorylated and translocated from the cytoplasm to the nucleus after heat shock (Geum et al., 2002). To further understand the distribution of p-HSP27 in MERRF cybrids after stress conditions and the correlation with cell viability, heat shock stress was applied to D5-1 and C5 cybrids. After 43℃ heat shock treatment for 30 min, cells were harvested and the cellular localization of p-HSP27 was visualized by immunofluorescence staining with antibody against specific p-HSP27. It is noted that HSP27 was mainly located in the cytoplasm before heat shock treatment. A large portion of p-HSP27 was translocated into the nucleus right after heat shock treatment. Next, we examined the cellular localization of p-HSP27 during recovery intervals. The heat shock treated cells under 43℃ for 30 min were then allowed to recover

from the heat shock for different time intervals. With prolonged recovery intervals, most of the p-HSP27 returned to the cytoplasm within 7 hr recovery in D5-1 but not in C5 mutant cybrids (Fig. 10). Based on this result, cell viability assays was performed by using PI staining to determine whether there is correlation between the nuclear-translocated p-HSP27 and apoptotic cells. Our results showed that a significant cell death of D5-1 cybrids appeared at 3 hr recovery and lasted to 9 hr receovery, when compared with no treatment control (Fig.11). Therefore, the nuclear-translocated p-HSP27 seems to correlate with cell viability during heat shock recovery in the normal cybrids. However, in the mutant C5 cybrids, with most of the p-HSP27 retained in the nucleus even after 9 hr recovery, a large scale of cell death was not observed until the prolonged recovery of 7 to 9 hr.

3.9 The oxidative stress induced nuclear DNA damage retains the p-HSP27 in the nucleus

In the previous study, the increased amount of ROS was observed in cultured cells harboring A8344G mutation of mtDNA (Liu et al., 2009). It

was suggested that mtDNA mutation-elicited oxidative stress and oxidative damage are involved in the pathogenesis and progression of MERRF disease (Wu et al., 2010). Moreover, It was speculated that the p-HSP27 entered the nucleus from the cytoplasm to perform a protective function (Geum et al., 2002; Bryantsev et al., 2007). Therefore, to investigate whether the nuclear-translocated p-HSP27 in C5 cybrids during prolonged recovery after heat shock treatment is due to damaged nDNA caused by oxidative stress, H_2O_2 was added to D5-1 cybrids for various time intervals and immunocytochemical staining was performed to examine the cellular localization of p-HSP27. As shown in Figure 12, when D5-1 cybrids were treated with 90μM H_2O_2 for 30 min, p-HSP27 was aggregated at the perinuclear region. Furthermore, with a prolonged treatment of 60 min, most of the p-HSP27 clearly entered the nucleus. Based on this observation, 90μM H_2O_2 for 60 min was used as the oxidative stress condition. Meanwhile, DNA fragmentation assay was performed. The DNA laddering was observed after 90μM H_2O_2 for 60 min (Figure. 13). After cells were treated with 90μM H_2O_2 for 60 min, cells were incubated in normal growth condition for different recovery periods and the cellular localization of p-HSP27 was examined. Our

results showed that the majority of p-HSP27 still retained in the nucleus even after prolonged recovery of 7 hr (Figure. 14). From the abovementioned, we suggest that the oxidative stress induced nDNA damage may be able to retain p-HSP27 in the nucleus.

4. ***Discussion***

Our previous data have shown a decreased HSP27 in the cells harboring A8344G point mutation on mtDNA (Chen et al., 2011). Because the ATP synthesis level decreased to 50 % of the control cells (Boulet et al., 1992). We then evaluated whether the decreased ATP level in the mutant cybrids leads to the decreased level of p-HSP27 by checking phosphorylated ERK (p-ERK) under the same growth conditions. However, Western blot analysis showed an increased p-ERK in the presence of A8344G mutation when compared to the normal control cells (Appendix Fig. 3). In addition, a significant increase of p-HSP27 was observed in mutant CPEO cells, which contained about 80% of 4977-bp deletion mtDNA (Liu et al., 2004). These results indicate that the reduced level of p-HSP27 is not due to a common effect of the low content of ATP in MERRF cells. It is known that HSP27 is phosphorylated by MAPK upon stresses and dephosphorylated by PP2A (Cairns et al., 1994; Berrou and Bryckaert, 2009). Therefore, we next tested whether the decreased p-HSP27 is due to defective kinase activity in MERRF cybrids by transient transfection analysis. The ratio of exo-pHSP27/exo- HSP27 was used to determine the

phosphorylation rate in cells with or without A8344G mutation. However, the ratios showed no significant difference between D5-1 and C5 (Fig. 1). Taken these results together, the decreased p-HSP27 in C5 cybrids may not be due to decreased ATP level nor the defective kinase and phosphatase activity.

It is known that HSP27 are phosphorylated by MAPK upon stresses and dephosphorylated by PP2A (Cairns et al., 1994; Berrou and Bryckaert, 2009). Given the fact that phosphorylation of HSP27 occurred within minutes under stress conditions, we wonder whether the reduced level of p-HSP27 in mutant MERRF cybrids has impact on the responses to stress conditions. Thus, heat shock and MG132 treatments were applied to the mutant and normal cybrids and Western blot analysis by using specific antibody against p-HSP27 was performed. Similar stress responses were observed in both D5-1 and C5 cybrids upon heat shock and MG132 treatments. Meanwhile, it is worth noting that under MG132 treatment, p-HSP27 was accumulated after 2 hr incubation. Because MG132 is a non-specific protease inhibitor, the accumulation of p-HSP27 indicates that the degradation of p-HSP27 is mediated by the ubiquitin-proteasome pathway. Nevertheless, our previous report has shown that the

degradation of HSP27 is through autophagy-lysosomal pathway (Chen et al., 2011). Because HSP27 formed large polymers but p-HSP27 showed a tendency to form dimers or tetramers (Kosten and Moens, 2009). Therefore, we speculate that different conformations of HSP27 may go through different degradation pathways.

It is known that HSP27 functions as a negative regulator of apoptosis (Rocchi et al., 2006; Pandey et al., 2000). In contrast, the decreased HSP27 in cells enhanced the apoptotic stress (Rocchi et al., 2006). We have shown an increased cell death in the mutant MERRF cybrids harboring reduced amount of HSP27 under apoptotic stress (Appendix Fig. 5). To further confirm whether the reduced level of the anti-apoptotic property of HSP27 may be responsible, at least in part, to disease cells becoming less viable under different stresses (Liu et al., 2004; Wu et al., 2010), we exogenously over-expressed HSP27 in mutant cybrids and the stable cells were then treated with STS to induce apoptosis. The results from Western blot assay showed significant decrease of activated caspase 3 in the HSP27 over-expressed stable lines, C5-C5 and C6, compared with C5, which contains no over-expressed HSP27. Our results are consistent with other reports that the over-expressed HSP27 reduces cell

death when cells are under stresses (Kim et al., 2010; Park et al., 2009). It is worth to note that the protein level of exogenous HSP27 is slightly increased in C6 compared with that of C5-C5 (Fig. 3), which may be responsible for the decreased activated caspase 3 detected in C6 cybrids. On the other hand, the mitochondrial membrane potential in MERRF patient' fibroblasts with 89% mutant mtDNA retained only 20 % of the control cells (Boulet et al., 1992). We further examined whether the over-expressed HSP27 rescues mitochondrial membrane potential by JC-1 staining. However, even though the over-expressed HSP27 slightly increases mitochondrial membrane potential but the difference is not significant compared to the control cells (Fig. 5).

To further investigate the importance of HSP27 phosphorylation on cell protective functions under stresses, mammalian expression plasmids pcDNA3-HA-HSP27-S3A and pcDNA3-HA-HSP27-S3D were constructed. It was reported that only the large aggregates of HSP27 were able to confer protection against ROS (Arrigo, 2001). Moreover, murine constitutive expressed non-phosphorylatable mutant Hsp25, with serine 15 and serine 86 replaced by alanine, significantly decreased the

intracellular levels of ROS and strongly increased the glutathione content (Pre´ villel1 et al., 1998). In contrast, HSP27 phosphoryaltion is required for injured sensory and motor neuron survival in rat (Benn et al., 2002). In the present study, HA-HSP27-S3A and HA-HSP27-S3D were constructed for comparison and transient transfection assay was performed to analyze the protective function of the mutant forms of HSP27 under STS treatment. Our results demonstrate that HA-HSP27-S3D transfected cells showed a significant decreased cell death under STS treatment when compared to that of the HA-HSP27-S3A transfected cells. Our results reveal the importance of p-HSP27 on the anti-apoptotic function in cybrid cells harboring A8344G mutation. On thither hand, we further investigated the correlation between the cellular localization of p-HSP27 and cell viability. Our previous results showed that HSP27 and p-HSP27 distributed evenly in the cytoplasm in both D5-1 and C5 under normal growth conditions (Appendix Fig. 2). In the present study, we find that p-HSP27 enters the nucleus immediately after heat shock and H_2O_2 treatment. However, it has been shown that the nuclear translocation of p-HSP27 is cell type specific. For example, Geum et al. reported constitutive entry of Hsp25 mutants mimicking

phosphorylation into nuclei of unstressed hippocampal neuron progenitor Cells while the endogenous HSP25 distributed evenly in the cytoplasm (Geum et al., 2002). Constitutive entry of Drosophila HSP27 into nuclei of developing oocytes has also been reported (Marin and Tanguay, 1996). In contrast, Adhikari et al. observed that both Hsp25 and related alpha-B crystallin were excluded from nuclei of mature myocytes, but not immature myoblasts, under all tested conditions, including heat shock (Adhikari et al., 2004). Moreover, Bryantsev et al. reported that the phosphorylation of HSP27 in necessary for nuclear translocation but not sufficiently. Other report also indicated that the p-HSP27 enters the nucleus for nucleic acid binding to reduce nDNA breakdown (Korber et al., 1999). In my study, a large portion of p-HSP27 was translocated into the nucleus right after heat shock treatment. With prolonged recovery intervals, most of the p-HSP27 returned to the cytoplasm within 7 hr recovery in D5-1 but not in C5 mutant cybrids (Fig. 10). We further assessed cell viability along with each treatment intervals. Our results show that a significant cell death of D5-1 cybrids appeared at 3 hr recovery and lasted to 9 hr recovery when compared with no treatment control. Therefore, the nuclear-translocated p-HSP27 seems to correlate

with cell viability during heat shock recovery in the normal cybrids. However, in the mutant C5 cybrids, with most of the p-HSP27 retained in the nucleus even after 9 hr recovery, a large scale of cell death was not observed until the prolonged recovery of 7 to 9 hr. It is noted that the increased amount of ROS was observed in cultured cells harboring A8344G mutation of mtDNA (Liu et al., 2009). It was suggested that mtDNA mutation-elicited oxidative stress and oxidative damage are involved in the pathogenesis and progression of MERRF disease (Wu et al., 2010). Therefore, we speculate that the pre-existed oxidative stress in C5 cybrids may be responsible for the delay but severe cell death in mutant cells. To verify the effects of oxidative stress on p-HSP27 distribution, H_2O_2 was added to D5-1 as an oxidative stress inducer and then cells were incubated in normal condition for recovery. Our results showed that the majority of p-HSP27 still retained in the nucleus even after a prolonged recovery of 7 hr, which is consistent with what observed in C5 mutant cells. We suggested that the oxidative stress induced nDNA damage may be able to retain p-HSP27 in the nuclei of mutant cybrids under stress condition. However, the prolong retention of the nuclear-translocated p-HSP27 eventually cannot reverse the global

defects induced by mutated mtDNA. Thus, a large scale of cell death was observed after 7 to 9 hr recovery.

In the previous studies, most of them have focused on the pathogenesis or the symptoms of the MERRF disease. However, in our laboratory, we are interested in investigating the correlation between HSP27 and MERRF disease cellular model. In the present study, we found that the drastically decreased p-HSP27 in cells bearing A8344G mtDNA mutation was not due to the defective kinase activity or the decreased ATP level. Additionally, the decreased p-HSP27 did not affect normal stress responses. Moreover, by examining mutant cells carrying non-phosphorylatable or phosphomimicking-HSP27, we observed that the phosphomimicking-HSP27 transfected cells especially show the ability to desensitize mutant cells to STS treatment, indicating the important protective function of p-HSP27 on mutant MERRF cybrids under apoptotic stress. Furthermore, we suggest that the nuclear-translocated p-HSP27 correlates with cell viability under stresses. In conclusion, this study provides evidence that the p-HSP27 plays very important roles in

the MERRF disease cellular model. We hope these findings will provide new insight into the therapeutic targets of the MERRF disease.

5.References

Adhikari, A.S., Rao, K.S., Rangaraj, N., Parnaik, V.K., and Rao, C.M. (2004). Heat stress-induced localization of small heat shock proteins in mouse myoblasts: intranuclear lamin A/C speckles as target for alpha B-crystallin and Hsp25. Experimental Cell Research *299*, 393-403.

Ahmad, S., Ahmad, A., Ghosh, M., Leslie, C.C., and White, C.W. (2004). Extracellular ATP-mediated signaling for survival in Hyperoxia-induced oxidative stress. Journal of Biological Chemistry *279*, 16317-16325.

Antonicka, H., Floryk, D., Klement, P., Stratilova, L., Hermanska, J., Houstkova, H., Kalous, M., Drahota, Z., Zeman, J., and Houstek, J. (1999). Defective kinetics of cytochrome *C* oxidase sold alteration of mitochondrial membrane potential in fibroblasts and cytoplasmic hybrid cells with the mutation for myoclonus epilepsy with ragged-red fibres ('MERRF') at position 8344 nt. Biochemical Journal *342*, 537-544.

Arpa, J., Campos, Y., GutierrezMolina, M., MartinCasanueva, M.A., CruzMartinez, A., PerezConde, M.C., LopezPajares, R., Morales, M.C., Tatay, J., Lacasa, T., *et al.* (1997). Gene dosage effect in one family with myoclonic epilepsy and ragged-red fibers (MERRF). Acta Neurologica Scandinavica *96*, 65-71.

Arya, R., Mallik, M., and Lakhotia, S.C. (2007). Heat shock genes - integrating cell survival and death. Journal of Biosciences *32*, 595-610.

Berrou, E., and Bryckaert, M. (2009). Recruitment of protein phosphatase 2A to dorsal ruffles by platelet-derived growth factor in smooth muscle cells: Dephosphorylation of Hsp27. Experimental Cell Research *315*, 836-848.

Boulet, L., Karpati, G., and Shoubridge, E.A. (1992). Distribution and threshold expression of the tRNA(Lys) mutation in skeletal muscle of patients with myoclonic epilepsy and ragged-red fibers (MERRF). American Journal of Human Genetics *51*, 1187-1200.

Bruey, J.M., Ducasse, C., Bonniaud, P., Ravagnan, L., Susin, S.A., Diaz-Latoud, C., Gurbuxani, S., Arrigo, A.P., Kroemer, G., Solary, E., *et al.* (2000). Hsp27 negatively regulates cell death by interacting with cytochrome c. Nature Cell Biology *2*, 645-652.

Bryantsev, A.L., Chechenova, M.B., and Shelden, E.A. (2007). Recruitment of phosphorylated small heat shock protein Hsp27 to nuclear speckles without stress. Experimental Cell Research *313*, 195-209.

Cairns, J., Qin, S.X., Philp, R., Tan, Y.H., and Guy, G.R. (1994). Dephosphorylation of the small heat-shock protein hsp27 in-vivo by protein phosphatase 2a. Journal of Biological Chemistry *269*, 9176-9183.

Charette, S.J., Lavoie, J.N., Lambert, H., and Landry, J. (2000). Inhibition of Daxx-mediated apoptosis by heat shock protein 27. Molecular and Cellular Biology *20*, 7602-7612.

Chen CY, C.H., Gi SJ, Chi TH, Cheng CK, Hsu CF, Ma YS, Wei YH, Liu CS, Hsieh M. (2011). Decreased heat shock protein 27 expression and altered autophagy in human cells harboring A8344G mitochondrial DNA mutation. Mitochondrion.

Chinnery, P.F., Howell, N., Lightowlers, R.N., and Turnbull, D.M. (1997). Molecular pathology of MELAS and MERRF - The relationship between mutation load and clinical phenotypes. Brain *120*, 1713-1721.

Concannon, C.G., Gorman, A.M., and Samalli, A. (2003). On the role of Hsp27 in regulating apoptosis. Apoptosis *8*, 61-70.

Crack, J., Mansour, M., and MacRae, T.H. (2000). Functional analysis of a developmentally regulated small heat shock/alpha-crystallin protein from Artemia franciscana. Molecular Biology of the Cell *11*, 2675.

Cuesta, R., Laroia, G., and Schneider, R.J. (2000). Chaperone Hsp27 inhibits translation during heat shock by binding eIF4G and facilitating dissociation of cap-initiation complexes. Genes & Development *14*, 1460-1470.

Ehrnsperger, M., Graber, S., Gaestel, M., and Buchner, J. (1997). Binding of non-native protein to Hsp25 during heat shock creates a reservoir of folding intermediates for reactivation. Embo Journal *16*, 221-229.

Garrido, C., Bruey, J.M., Fromentin, A., Hammann, A., Arrigo, A.P., and Solary, E. (1999). HSP27 inhibits cytochrome *C*-dependent activation of procaspase-9. Faseb Journal *13*, 2061-2070.

Geum, D., Son, G.H., and Kim, K. (2002). Phosphorylation-dependent cellular localization and thermoprotective role of heat shock protein 25 in hippocampal progenitor cells. Journal of Biological Chemistry *277*, 19913-19921.

Ghosh, A., Chawla-Sarkar, M., and Stuehr, D.J. (2011). Hsp90 interacts with inducible NO synthase client protein in its heme-free state and then drives heme insertion by an ATP-dependent process. Faseb Journal *25*, 2049-2060.

Grossin, L., Etienne, S., Gaborit, N., Pinzano, A., Cournil-Henrionnet, C., Gerard, C., Payan, E., Netter, P., Terlain, B., and Gillet, P. (2004). Induction of heat shock protein 70 (Hsp70) by proteasome inhibitor MG 132 protects articular chondrocytes from cellular death in vitro and in vivo. Biorheology *41*, 521-534.

Hammans, S.R., Sweeney, M.G., Brockington, M., Lennox, G.G., Lawton, N.F., Kennedy, C.R., Morganhughes, J.A., and Harding, A.E. (1993). The mitochondrial-DNA transfer RNA(Lys) A- G(8344) mutation and the syndrome of myoclonic epilepsy with ragged-red fibers (MERRF) - relationship of clinical phenotype to proportion of mutant mitochondrial-DNA. Brain *116*, 617-632.

Hickey, E., Brandon, S.E., Sadis, S., Smale, G., and Weber, L.A. (1986). Molecular-cloning of sequences encoding the human heat-shock proteins and their expression during hyperthermia. Gene *43*, 147-154.

Huot, J., Houle, F., Marceau, F., and Landry, J. (1997). Oxidative stress-induced actin reorganization mediated by the p38 mitogen-activated protein kinase heat shock protein 27 pathway in vascular endothelial cells. Circulation Research *80*, 383-392.

Jakob, U., Gaestel, M., Engel, K., and Buchner, J. (1993). SMALL HEAT-SHOCK PROTEINS ARE MOLECULAR CHAPERONES. Journal of Biological Chemistry *268*, 1517-1520.

James, A.M., Wei, Y.H., Pang, C.Y., and Murphy, M.P. (1996). Altered mitochondrial function in fibroblasts containing MELAS or MERRF mitochondrial DNA mutations. Biochemical Journal *318*, 401-407.

Kanagasabai, R., Karthikeyan, K., Vedam, K., Qien, W., Zhu, Q.Z., and Ilangovan, G. (2010). Hsp27 Protects Adenocarcinoma Cells from UV-Induced Apoptosis by Akt and p21-Dependent Pathways of Survival. Molecular Cancer Research *8*, 1399-1412.

Kim, M., Park, S.W., Chen, S.W.C., Gerthoffer, W.T., D'Agati, V.D., and Lee, H.T. (2010). Selective renal overexpression of human heat shock protein 27 reduces renal ischemia-reperfusion injury in mice. American Journal of Physiology-Renal Physiology *299*, F347-F358.

Korber, P., Zander, T., Herschlag, D., and Bardwell, J.C.A. (1999). A new heat shock protein that binds nucleic acids. Journal of Biological Chemistry *274*, 249-256.

Kostenko, S., and Moens, U. (2009). Heat shock protein 27 phosphorylation: kinases, phosphatases, functions and pathology. Cellular and Molecular Life Sciences *66*, 3289-3307.

Larsson, N.G., Tulinius, M.H., Holme, E., Oldfors, A., Andersen, O., Wahlstrom, J., and Aasly, J. (1992). Segregation and manifestations of the mtDNA trans rnalys A-G(8344) mutation of myoclonus epilepsy and ragged-red fibers (MERRF) syndrome. American Journal of Human Genetics *51*, 1201-1212.

Lenz, G., Goncalves, D., Luo, Z.J., Avruch, J., Rodnight, R., and Neary, J.T. (2001). Extracellular ATP stimulates an inhibitory pathway towards growth factor-induced cRaf-1 and MEKK activation in astrocyte cultures. Journal of Neurochemistry *77*, 1001-1009.

Liu, C.Y., Lee, C.F., Hong, C.H., and Wei, Y.H. (2004). Mitochondrial DNA mutation and depletion increase the susceptibility of human cells to apoptosis. In Mitochondrial Pathogenesis: from Genes and Apoptosis to Aging and Disease, H.K. Lee, S. DiMauro, M. Tanaka, and Y.H. Wei, eds., pp. 133-145.

Loktionova, S.A., and Kabakov, A.E. (2001). Phosphatase inhibitors prevent HSP27 dephosphorylation, destruction of stress fibrils, and morphological changes in endothelial cells during ATP depletion. Bulletin of Experimental Biology and Medicine *132*, 914-917.

Marin, R., and Tanguay, R.M. (1996). Stage-specific localization of the small heat shock protein Hsp27 during oogenesis in Drosophila melanogaster. Chromosoma *105*, 142-149.

Matsushima-Nishiwaki, R., Takai, S., Adachi, S., Minamitani, C., Yasuda, E., Noda, T., Kato, K., Toyoda, H., Kaneoka, Y., Yamaguchi, A., *et al.* (2008). Phosphorylated heat shock protein 27 represses growth of hepatocellular carcinoma via inhibition of extracellular signal-regulated kinase. Journal of Biological Chemistry *283*, 18852-18860.

Morano, K.A., and Thiele, D.J. (1999). Heat shock factor function and regulation in response to cellular stress, growth, and differentiation signals. Gene Expression *7*, 271-282.

Panasenko, O.O., Seit-Nebi, A., Bukach, O.V., Marston, S.B., and Gusev, N.B. (2002). Structure and properties of avian small heat shock protein with molecular weight 25 kDa. Biochimica Et Biophysica Acta-Proteins and Proteomics *1601*, 64-74.

Pandey, P., Farber, R., Nakazawa, A., Kumar, S., Bharti, A., Nalin, C., Weichselbaum, R., Kufe, D., and Kharbanda, S. (2000). Hsp27 functions as a negative regulator of cytochrome c-dependent activation of procaspase-3. Oncogene *19*, 1975-1981.

Park, S.W., Chen, S.W.C., Kim, M., D'Agati, V.D., and Lee, H.T. (2009). Human heat shock protein 27-overexpressing mice are protected against acute kidney injury after hepatic ischemia and reperfusion. American Journal of Physiology-Renal Physiology *297*, F885-F894.

Pirkkala, L., Nykanen, P., and Sistonen, L. (2001). Roles of the heat shock transcription factors in regulation of the heat shock response and beyond. Faseb Journal *15*, 1118-1131.

Preville, X., Schultz, H., Knauf, U., Gaestel, M., and Arrigo, A.P. (1998). Analysis of the role of Hsp25 phosphorylation reveals the importance of the oligomerization state of this small heat shock protein in its protective function against TNF alpha- and hydrogen peroxide-induced cell death. Journal of Cellular Biochemistry *69*, 436-452.

Rocchi, P., Jugpal, P., So, A., Sinneman, S., Ettinger, S., Fazli, L., Nelson, C., and Gleave, M. (2006). Small interference RNA targeting heat-shock protein 27 inhibits the growth of prostatic cell lines and induces apoptosis via caspase-3 activation in vitro. Bju International *98*, 1082-1089.

Rossignol, R., Faustin, B., Rocher, C., Malgat, M., Mazat, J.P., and Letellier, T. (2003). Mitochondrial threshold effects. Biochemical Journal *370*, 751-762.

Schon, E.A., Bonilla, E., and DiMauro, S. (1997). Mitochondrial DNA mutations and pathogenesis. Journal of Bioenergetics and Biomembranes *29*, 131-149.

Tak, H., Jang, E., Kim, S.B., Park, J., Suk, J., Yoon, Y.S., Ahn, J.K., Lee, J.H., and Joe, C.O. (2007). 14-3-3epsilon inhibits MK5-mediated cell migration by disrupting F-actin polymerization. Cellular Signalling *19*, 2379-2387.

Wei, Y.H., Kao, S.H., and Lee, H.C. (1996). Simultaneous increase of mitochondrial DNA deletions and lipid peroxidation in human aging. In Pharmacological Intervention in Aging and Age-Associated Disorders - Proceedings of the Sixth Congress of the International Association of Biomedical Gerontology, K. Kitani, A. Aoba, and S. Goto, eds., pp. 24-43.

Welch, W.J. (1993). Heat-shock proteins functioning as molecular chaperones - their roles in normal and stressed cells. Philosophical Transactions of the Royal Society of London Series B-Biological Sciences *339*, 327-333.

Yoneda, M., Miyatake, T., and Attardi, G. (1994). Complementation of mutant and wild-type human mitochondrial DNAs coexisting since the mutation event and lack of complementation of DNAs introduced separately into a cell within distinct organelles. Molecular and Cellular Biology *14*, 2699-2712.

6.Figures

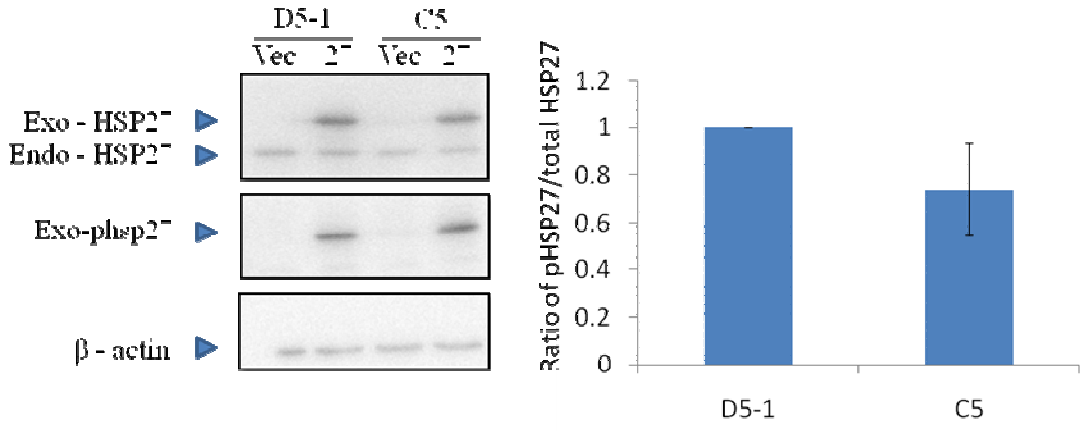

Fig. 1. Protein expression levels of transiently expressed HSP27 and p-HSP27 in the cybrids harboring A83449G mutation OF mtDNA and the normal control.

Protein expression level was analyzed by Western blot after HSP27-Myc-His plasmids were transfected into D5-1 and C5. The ratio of p-HSP27 /HSP27 revealed the protein phosphorylated level. Data are expressed as means ± SEM from 5 independent experiments.

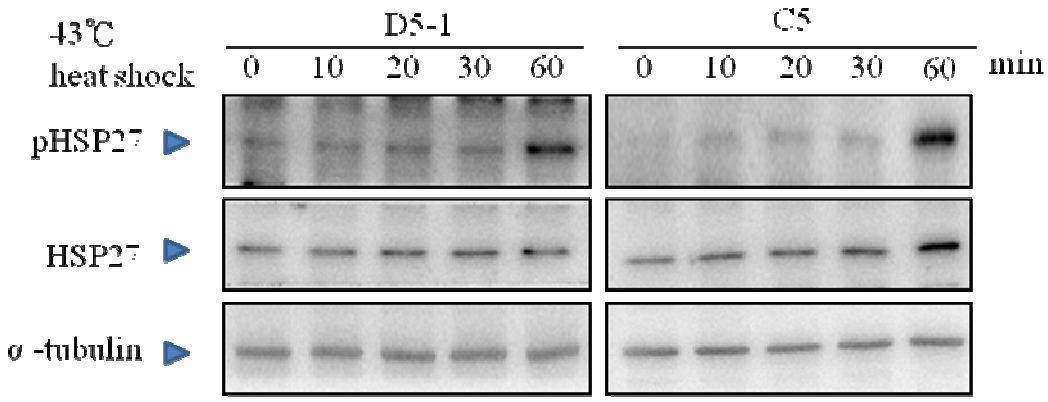

Fig. 2. Western blot analysis of p-HSP27 in the cybrids with or without A8344G mutation under heat shock treatment.

Cells were treated with heat shock at 43℃ with different time intervals. A significant increase of p-HSP27 was detected 60 min after 43 ℃ treatment in both normal and mutant cybrids. The protein expression level was analyzed by Western blot.

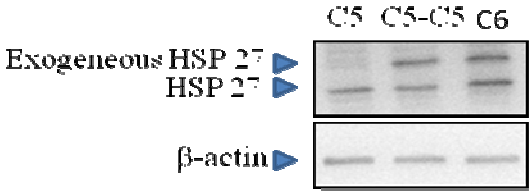

Fig. 3. Protein expression of exogenous HSP27 in cybrid clones harboring over-expressed HSP27.

C5-C5 and C6 were stably transfected with pcDNA3.1- HSP27-Myc-His from parental MERRF C5.The protein expression level was analyzed by Western blot.

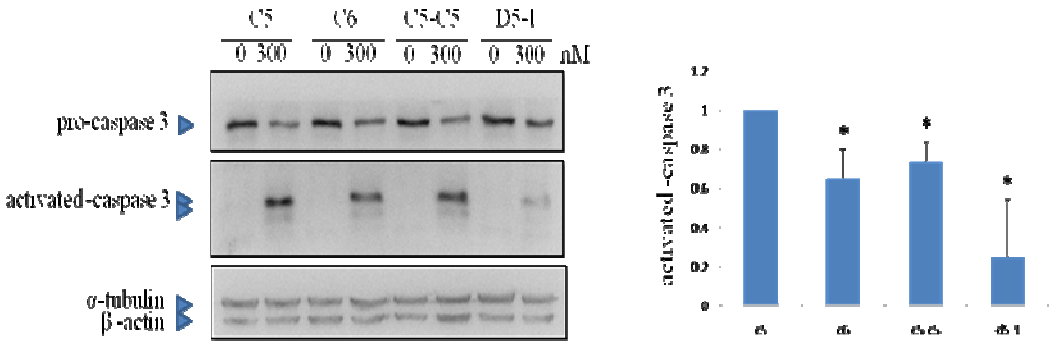

Fig. 4. Over-expression of HSP27 desensitized mutant cybrids to apoptotic stress.

Cybrid clones D5-1, C5, C5-C5 and C6 were treated with 300nM STS for 3 hr. The activated caspase 3 was used for the indication of apoptosis. Western blot analysis demonstrated that the levels of activated caspase 3 were suppressed by over-expression of HSP27 in stable clones C5-C5 and C6. The data are expressed as mean ± SEM from 5 independent experiments. *, $p < 0.05$ stable clones vs. C5.

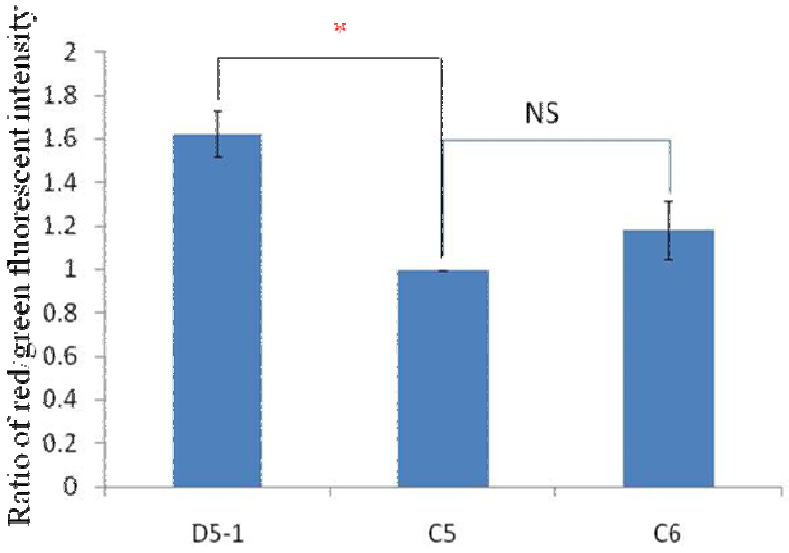

Fig. 5. The over-expressed HSP27 in the mutant MERRF cells did not rescue mitochondrial membrane potential.

Mitochondrial membrane potential was assayed by JC-1 staining. Cybrid clones C5-1, C5 and C6 were used for comparison. The ratio of red/green fluorescent intensity was the indication of mitochondrial membrane potential. Normal cybrids showed a significant increased level of the ratio of fluorescent intensity, when compared to mutant C5 and C6 clones.The data are expressed as mean ± SEM from over 200 cells counted from 20 different fields of two independent experiments. *, $p < 0.05$. NS = no significant.

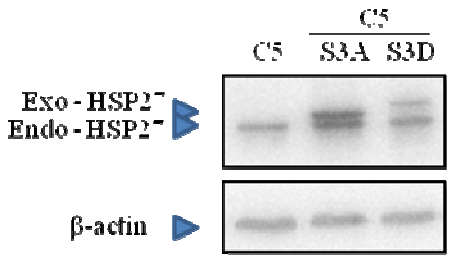

Fig. 6. Protein expression of point-mutated HSP27 in cybrids harboring A8344G mutation. Protein expression levels of HSP27 were analyzed by Western blot after C5 cybrids were transfected with the point-mutated HSP27 plasmids.

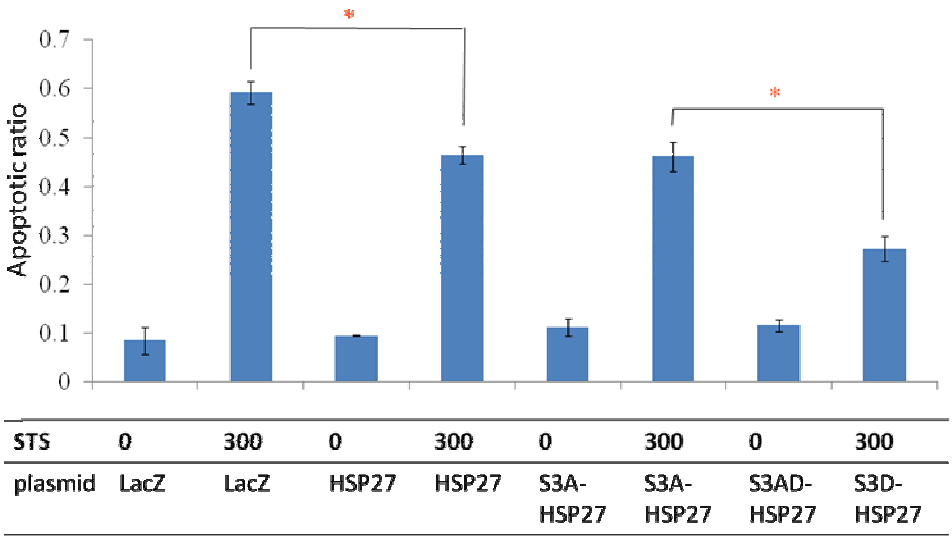

Fig. 7. The phosphomimicking-HSP27 desensitized mutant cybrids to the apoptotic stress induced by STS.

Cell viability assay was performed after C5 cybrids were transfected with point mutated HSP27 (HSP27-S3A, HSP27-S3D), wild type HSP27 and LacZ control. 24 hrs after transfection, cells were treated with 300nM STS for 3 hr and then immunofluorescently stained with anti–HA to detect positively transfected cells and PI staining was used for detection of nuclear fragmentation. Apoptotic cell ratios were obtained by counting more than 300 positively transfected cells from at least 10 different fields of three independent experiments.

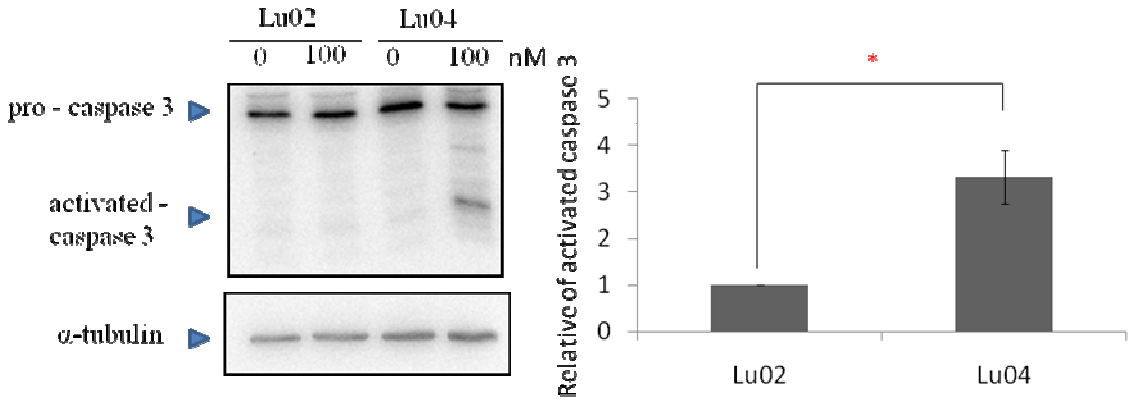

Fig. 8. Cells harboring A3243G mtDNA mutation elicited cell apoptosis under STS treatment.

Cybrid clones Lu02 and Lu04 were treated with 100nM STS for 6 hr. The activated caspase 3 was used for the indication of apoptosis. Western blot analysis demonstrated that the levels of activated caspase 3 were decreased in the normal cybrids Lu02. The data are expressed as mean ± SEM from 3 independent experiments. *, $p < 0.05$ stable clones vs. Lu02.

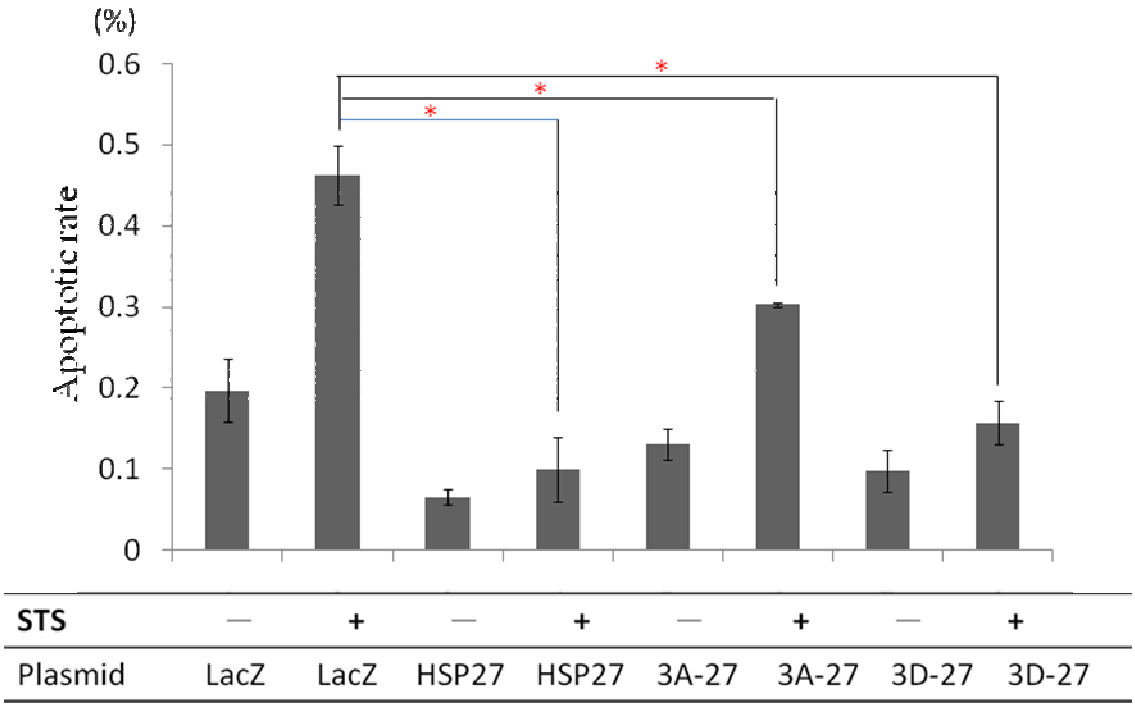

Fig. 9. The phosphomimicking-HSP27 desensitized mutant cybrids(Lu04) to the apoptotic stress induced by STS.

Cell viability assay was performed after Lu04 cybrids were transfected with point mutated HSP27 (HSP27-S3A, HSP27-S3D), wild type HSP27 and LacZ control. 24 hrs after transfection, cells were treated with 100nM STS for 6 hr and then immunofluorescently stained with anti–HA to detect positively transfected cells and PI staining was used for detection of nuclear fragmentation. Apoptotic cell ratios were obtained by counting more than 300 positively transfected cells from at least 10 different fields of three independent experiments.

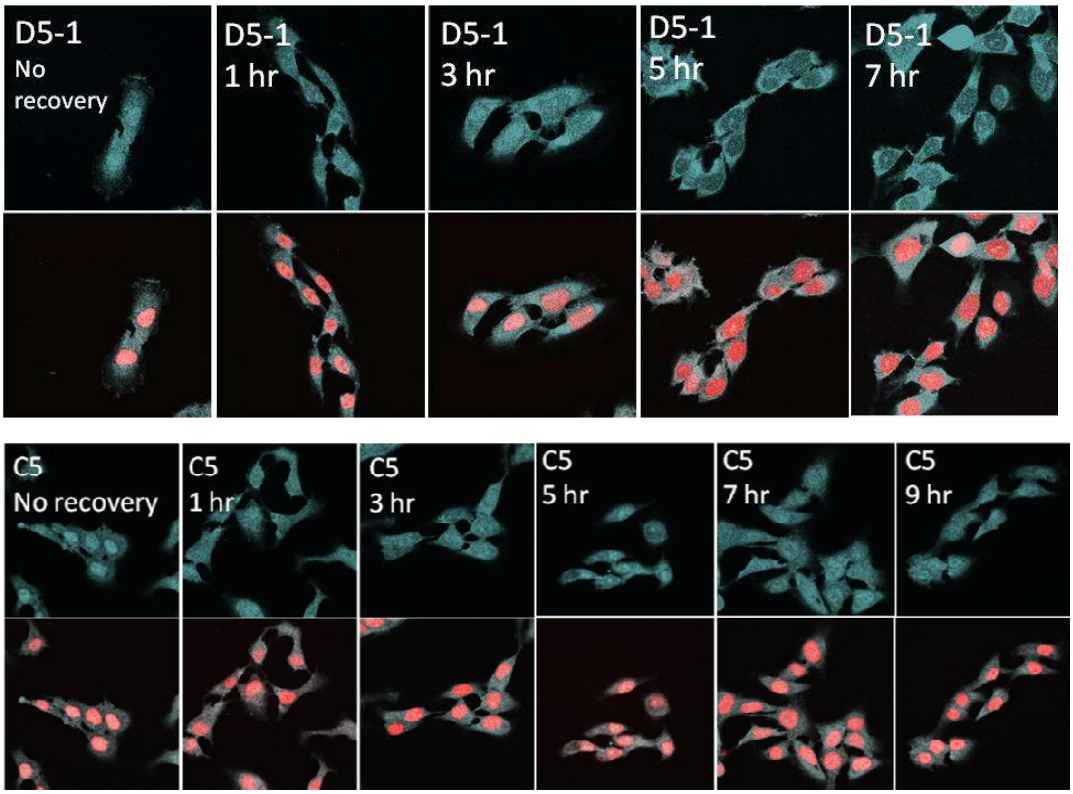

Fig. 10. The cellular localization of p-HSP27 in cybrids under heat shock treatment with and without A8344G mutation.

D5-1 and C5 cybrids were heat shocked at 43℃for 30 minutes and then incubated at 37℃ for 0, 1, 3, 5, 7 and 9 hr for recovery. The p-HSP27 entered the nucleus form the cytoplasm immediately after heat shock treatment. However, with prolonged recovery intervals the p-HSP27 returned to the cytoplasm in D5-1 cybrids but not in C5 cybrids. PI was used for nucleus staining.

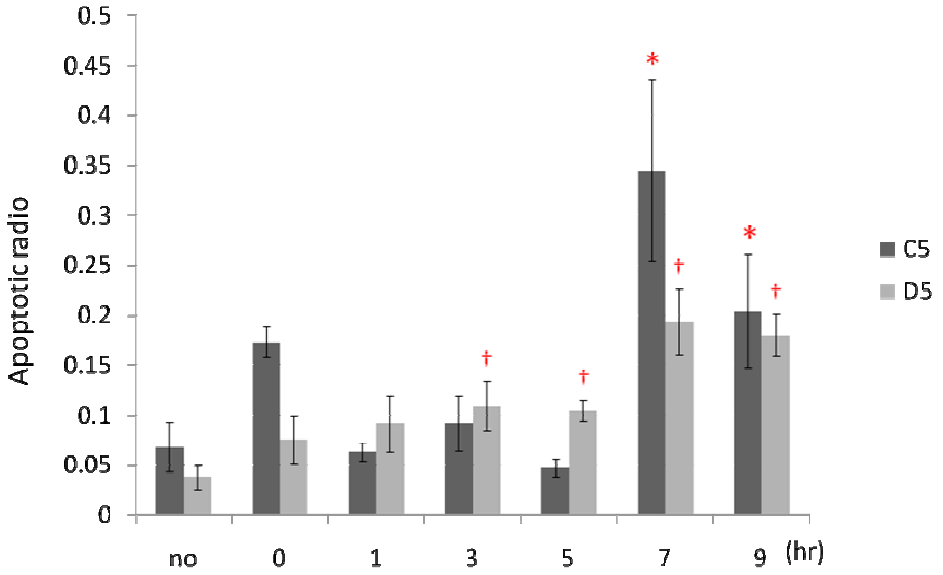

Fig. 11. Cell viability after heat shock treatment and different recovery intervals.

D5-1 and C5 cells were heat shocked at 43℃ for 30 min and recovered at 37℃ for 0, 1, 3, 5, 7 and 9 hrs. Apoptotic cells were counted after PI staining. There was a significant cell death in D5-1 cybrids from 3 hr to 9hr recovery after heat shock. But in C5 cybrids, a significant cell death was observed later until 7hr to 9 hr. The data are expressed as means ± SEM of from 3 independent experiments. More than 300 cells were counted from at least 10 different fields of three independent experiments. *, †, $p < 0.05$ vs. the no treatment control.

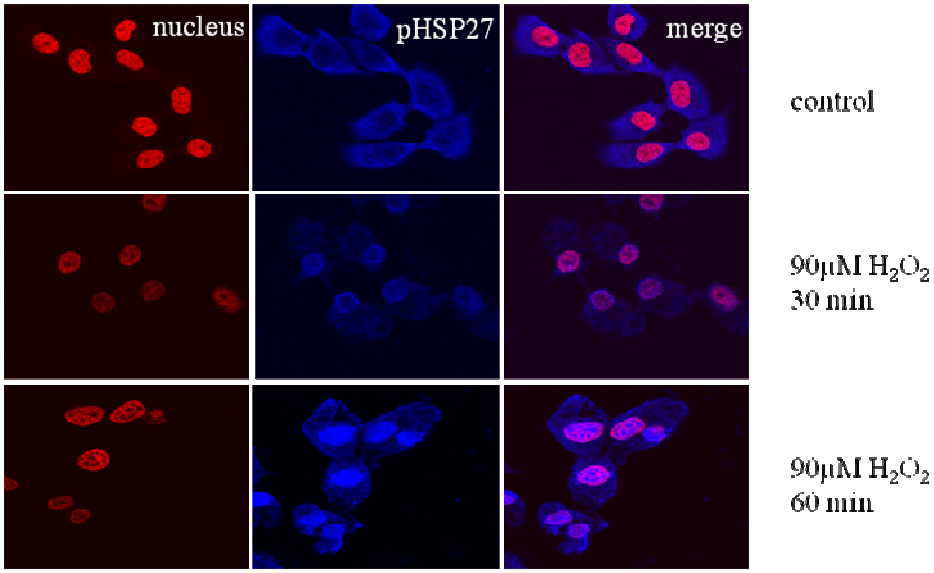

Fig. 12. Cellular localization of p-HSP27 after H_2O_2 treatment in D5-1 cybrids.

D5-1 cells were treated with 90μM H_2O_2 for 0, 30 and 60 min and immunofluorescent staining was performed with anti-pHSP27 antibody. p-HSP27 showed a strong signal at perinuclear region at 30 min treatment and then p-HSP27 entered the nucleus at 60 min. PI was used for nuclear staining.

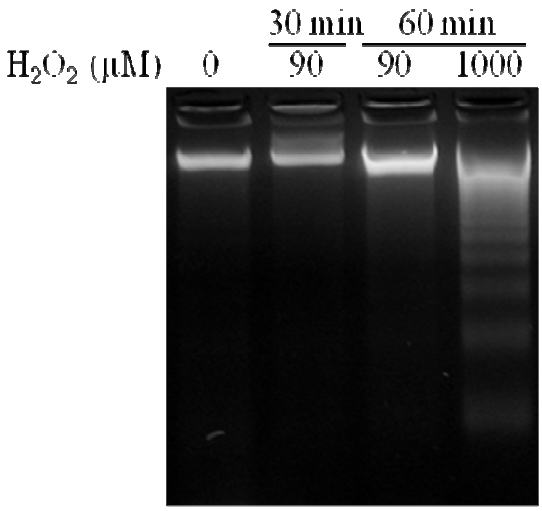

Fig. 13. DNA fragmentation assay in D5-1 after H_2O_2 treatment.

D5-1 cells were treated with 90μM H_2O_2 for 0, 30 and 60 min and a positive control of 1000μM H_2O_2 for 60 min. The DNA laddering was observed after 90μM H_2O_2 for 60 min.

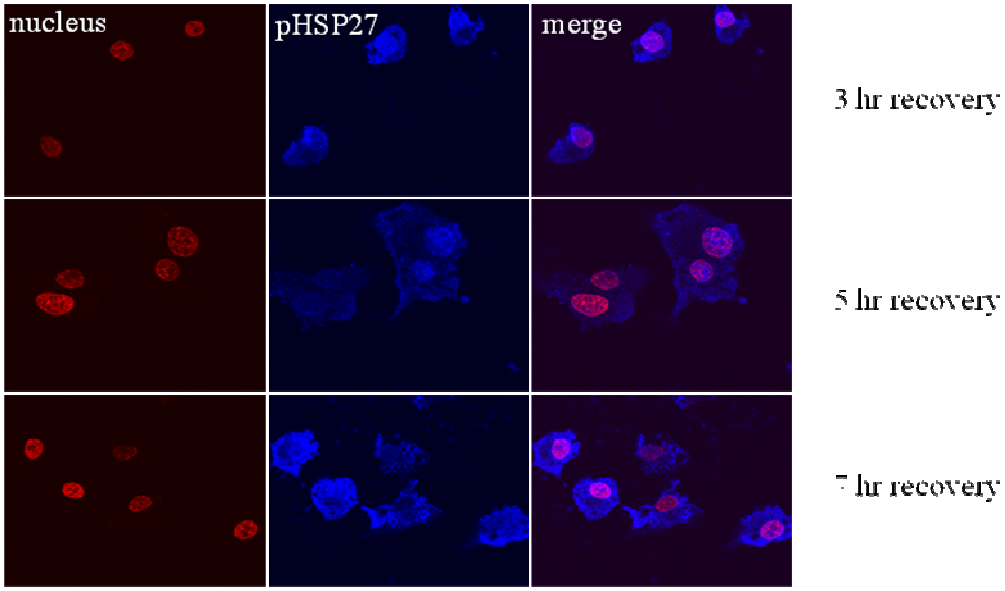

Fig. 14. The cellular localization of p-HSP27 after H_2O_2 treatment in D5-1 cybrids with different recovery intervals.

D5-1 cells were treated with 90μM H_2O_2 for 1 hr, and recovered at normal growth media for 3, 5 and 7 hrs. At each time point, immunofluorescent staining was performed with anti-pHSP27 antibody. Even prolonged recovery of 7 hr, p-HSP27 retained an intense signal in the nucleus. PI was used for nuclear staining.

7. Appendix figures

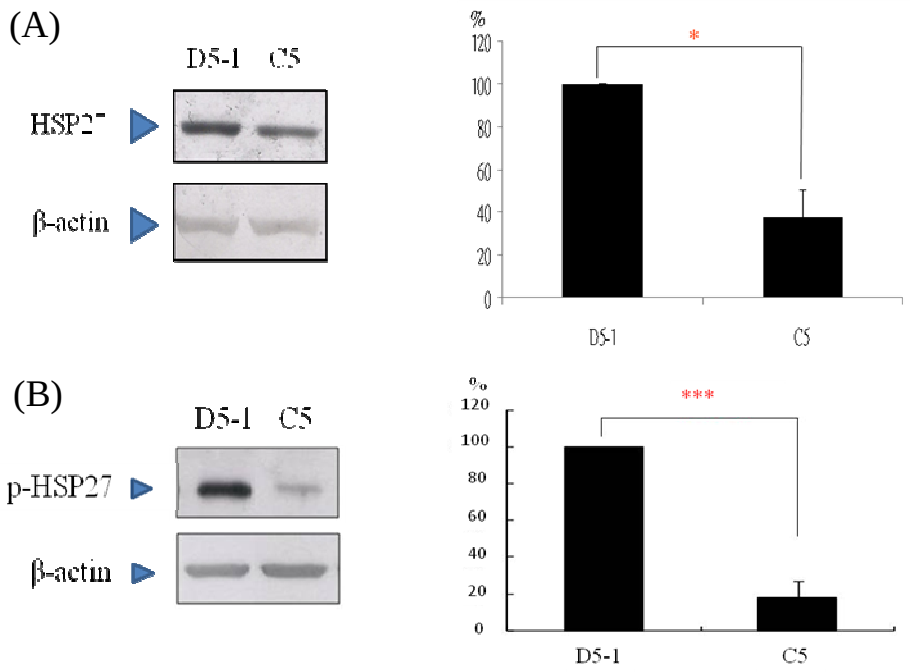

Appendix 1. Decreased protein expression of HSP27 and p-HSP27 in the cybrids harboring A8344G mtDNA mutation.

Both p-HSP27 and HSP27 showed a significant decrease in C5 cybrids. β-actin was used as an internal control. Data are expressed as mean ± SEM from 5 independent experiments. *, $p < 0.05$, mutant cybrids vs. the normal control

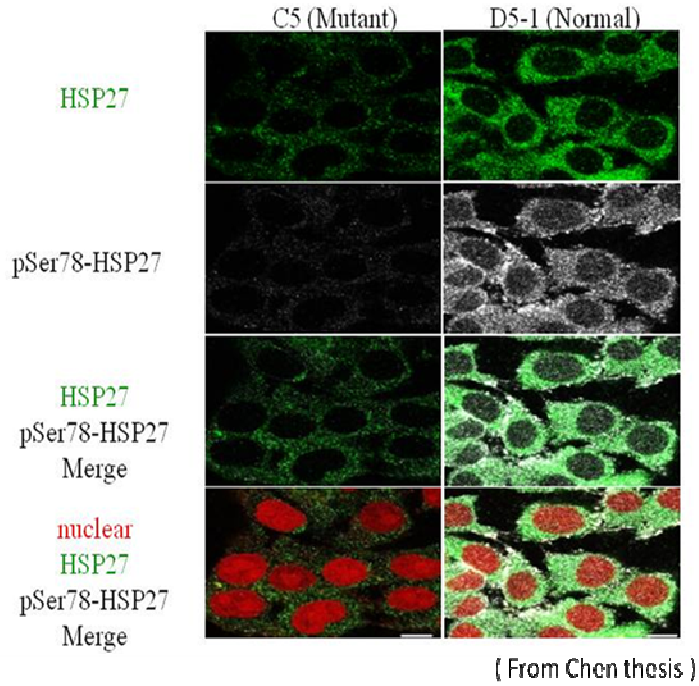

Appendix 2. Cellular localization of HSP27 and p-HSP27 in normal and MERRF cybrids. HSP27 and p-HSP27 are evenly distributed in the cytoplasm in both normal and MERRF cybrids under normal condition.

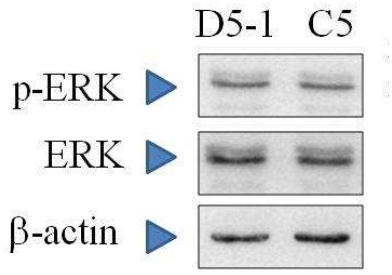

Appendix 3. Western blot analysis of ERK and p-ERK in the cybrids with or without A8344G.

Expression levels of ERK and p-ERK were determined by immunoblotting in whole-cell lysates from the wild type control cybrids (D5-1) or cybrids harboring A8344G mutation of mtDNA (C5). Following SDS-PAGE and Western blotting, ERK and p-ERK were detected by probing with appropriate antibodies. Anti-β-actin was added as an internal control.

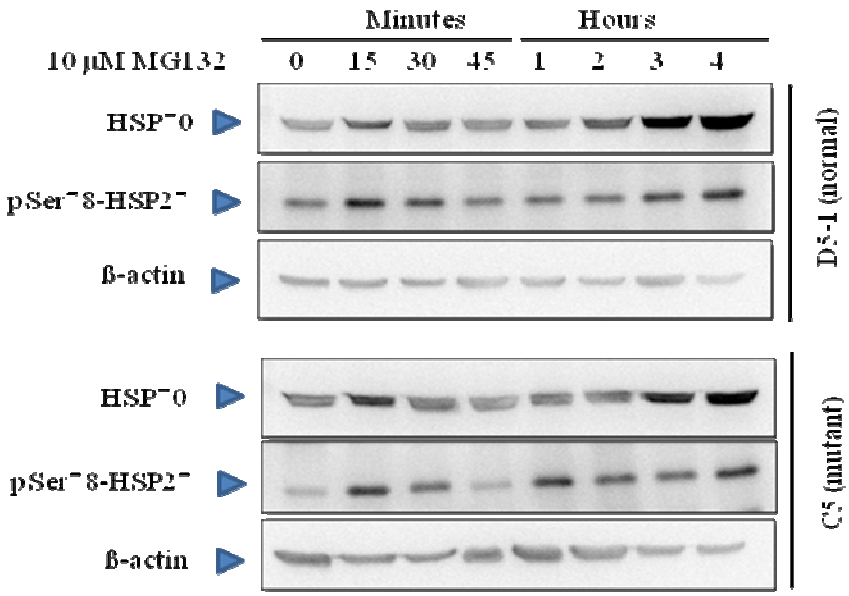

Appendix 4. Western blot analysis of p-HSP27 and HSP70 in the cybrids with or without A8344G mutation under MG132 treatment.

Expression levels of p-HSP27 and HSP70 were determined by immunoblotting in whole-cell lysates from the wild type control cybrids (D5-1) or cybrids harboring A8344G mutation of mtDNA (C5). Cells were treated with 10 μM MG132 for various time intervals as indicated. Following SDS-PAGE and Western blotting, p-HSP27 and HSP70 were detected by probing with appropriate antibodies. Anti-β-actin was added as an internal control.

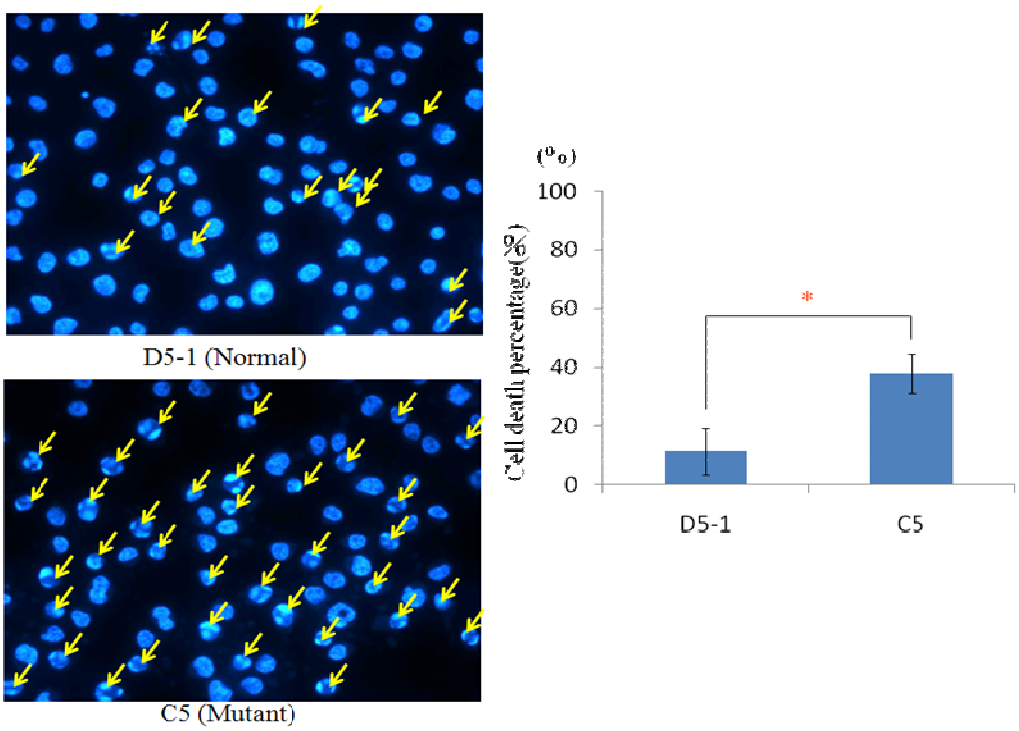

Appendix 5. Cells harboring A8344G mtDNA mutation elicited cell apoptosis under STS treatment.

Cell viability assay was performed after cells were treated with 400 nM STS for 2.5 hr and then stained with DAPI for of nuclear fragmentation.

(A)

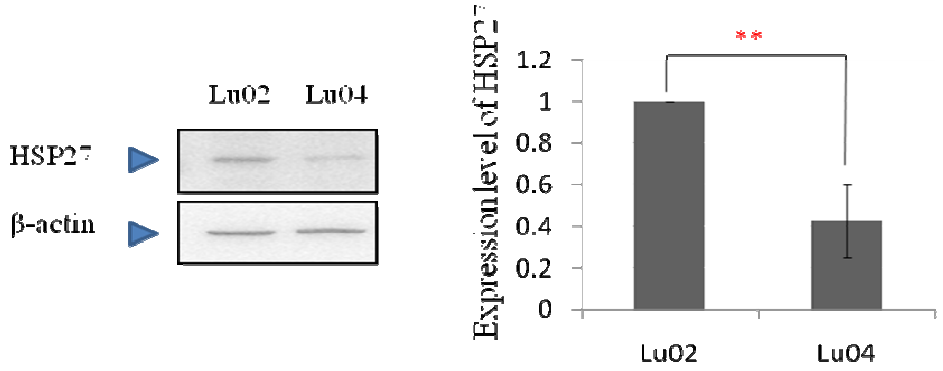

(B)

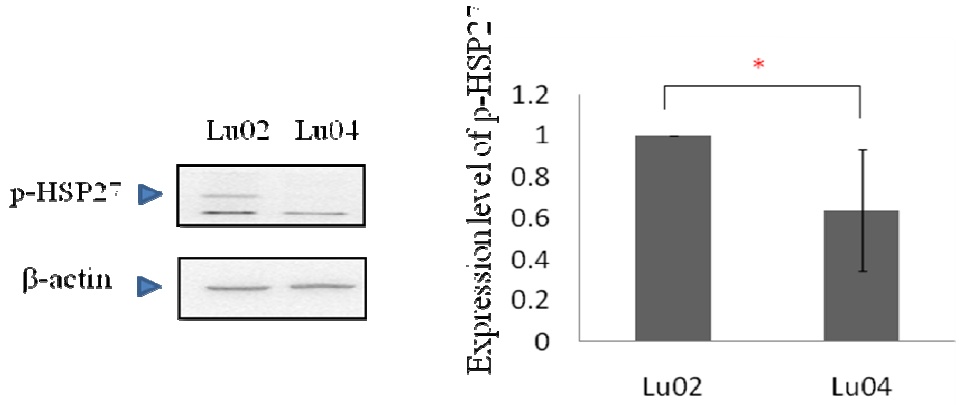

Appendix 6. Decreased protein expression of HSP27 and p-HSP27 in the cybrids harboring A3243G mtDNA mutation.

Both p-HSP27 and HSP27 showed a significant decrease in Lu04 cybrids. β-actin was used as an internal control. Data are expressed as mean ± SEM from 3 independent experiments. *, $p < 0.05$, mutant cybrids vs. the normal control